

**ASPEDAMITE, IDEALLY  $\square_{12}(\text{Fe}^{3+}, \text{Fe}^{2+})_3\text{Nb}_4[\text{Th}(\text{Nb}, \text{Fe}^{3+})_{12}\text{O}_{42}]\{(\text{H}_2\text{O}), (\text{OH})\}_{12}$ ,  
 A NEW HETEROPOLYNIOBATE MINERAL SPECIES  
 FROM THE HERREBØKASA QUARRY, ASPEDAMMEN, ØSTFOLD,  
 SOUTHERN NORWAY: DESCRIPTION AND CRYSTAL STRUCTURE**

MARK A. COOPER, YASSIR A. ABDU, NEIL A. BALL, PETR ČERNÝ AND FRANK C. HAWTHORNE<sup>§</sup>

*Department of Geological Sciences, University of Manitoba, Winnipeg, Manitoba R3T 2N2, Canada*

ROY KRISTIANSEN

*P.O. Box 32, N-1650 Sellebakk, Norway*

**ABSTRACT**

Aspedamite, ideally  $\square_{12}(\text{Fe}^{3+}, \text{Fe}^{2+})_3\text{Nb}_4[\text{Th}(\text{Nb}, \text{Fe}^{3+})_{12}\text{O}_{42}]\{(\text{H}_2\text{O}), (\text{OH})\}_{12}$ , is a new heteropoly niobate mineral species from the Herrebøkasa quarry, Aspedammen, Østfold, southern Norway. It occurs as small euhedral crystals of dodecahedra and cubes to a maximum of 50  $\mu\text{m}$  across, perched on a white mat of an Al–Nb–Fe–Ti–Ca–K-bearing silicate on a partly altered 12  $\times$  12  $\times$  6 mm crystal of monazite penetrated by plates of columbite–(Fe) and muscovite. Aspedamite is brownish orange with a very pale orange streak and an adamantine luster; it does not fluoresce under ultraviolet light. The Mohs hardness is 3–4, and it is brittle with a hackly fracture. The calculated density is 4.070 g/cm<sup>3</sup>, and the calculated index of refraction is 2.084. Aspedamite is cubic, space group  $Im\bar{3}$ ,  $a$  12.9078(6) Å,  $V$  2150.6(3) Å<sup>3</sup>,  $Z$  = 2. The strongest seven lines in the X-ray powder-diffraction pattern [ $d$  in Å( $l$ ) $hkl$ ] are: 9.107(100)011, 2.635(36)224, 2.889(33)024, 1.726(29)246, 3.233(28)004, 3.454(18)123, 4.567(15)022. A chemical analysis with an electron microprobe gave  $\text{Nb}_2\text{O}_5$  65.64,  $\text{Ta}_2\text{O}_5$  1.78,  $\text{SiO}_2$  0.78,  $\text{ThO}_2$  5.64,  $\text{TiO}_2$  2.15,  $\text{Fe}_2\text{O}_3$  10.56,  $\text{FeO}$  2.73,  $\text{MnO}$  0.82,  $\text{CaO}$  0.28,  $\text{K}_2\text{O}$  0.16,  $\text{La}_2\text{O}_3$  0.52,  $\text{Ce}_2\text{O}_3$  1.62,  $\text{Nd}_2\text{O}_3$  0.44,  $\text{H}_2\text{O}$  (calc.) 7.20, sum 100.32 wt.%; the  $\text{H}_2\text{O}$  content was determined by crystal-structure analysis. The empirical formula of aspedamite on the basis of 54 anions with  $\text{Fe}^{3+}/(\text{Fe}^{3+} + \text{Fe}^{2+}) = 0.67$  (estimated from crystal-chemical arguments) and  $\text{O}(4) = (\text{H}_2\text{O})_9 + (\text{OH})_3$  is  $\text{K}_{0.09}\text{Ca}_{0.13}\text{Ce}_{0.26}\text{La}_{0.08}\text{Nd}_{0.07}\text{Fe}^{2+}_{1.00}\text{Mn}_{0.30}\text{Fe}^{3+}_{3.48}\text{Th}_{0.56}\text{Ti}^{4+}_{0.71}\text{Si}_{0.34}\text{Nb}_{12.98}\text{Ta}_{0.21}\text{O}_{42}(\text{H}_2\text{O})_9(\text{OH})_3$ . The crystal structure of aspedamite was solved by direct methods and refined to an  $R_1$  index of 1.6% based on 596 observed reflections collected on a three-circle rotating-anode ( $\text{MoK}\alpha$  X-radiation) diffractometer equipped with multilayer optics and an APEX-II detector. The structure is based on the heteropolyanion  $[\text{DA}_{12}\text{O}_{42}]$  ( $D$  = Th, sum  $A$  = Nb<sub>9</sub>Fe<sup>3+</sup><sub>2</sub>Ti), which consists of twelve face- and corner-sharing  $\text{AO}_6$  octahedra that surround the [12]-coordinated  $D$  cation. There are eight heteropolyanions at the corners of the unit cell, with an additional heteropolyanion at the center, forming an  $I$ -centered arrangement. Each heteropolyhedral cluster is decorated by eight  $B$  octahedra, each of which bridges two adjacent clusters along the body diagonals of the cell. Further intercluster linkage is provided by the  $C$  octahedra, which link pairs of adjacent clusters in the  $\mathbf{a}$  direction. Aspedamite is isostructural with menezesite.

**Keywords:** aspedamite, new mineral species, heteropoly niobate, crystal structure, electron-microprobe analysis, optical properties, X-ray powder-diffraction pattern, Herrebøkasa quarry, Aspedammen, Østfold, Norway.

**INTRODUCTION**

The granite pegmatite quarry at Herrebøkasa is close to the small village of Aspedammen, south of the town of Halden on the southeastern side of Oslo Fjord, close to the eastern border of Sweden. The quarry is known for its well-developed crystals of monazite–(Ce), columbite–(Fe) and bertrandite. Examination of partly altered crystals of monazite showed microcrystals and crusts of secondary minerals, including rhabdophane–(Ce) that occurs as rusty brown fans, together with several

unknown Th-bearing phases. One small crystal of monazite was found to be partly covered by a white mat of an Al–Nb–Fe–Ti–Ca–K-bearing silicate on which were perched very tiny brownish orange dodecahedra and cubes of an unknown phase. Subsequent EDS–SEM analysis showed it to be an Fe–Ti–Th-bearing niobate. Further work confirmed that these grains are a new mineral species.

The mineral is named *aspедакмит* after the locality, close to Aspedammen. The new mineral and mineral name have been approved by the Commission on New

<sup>§</sup> E-mail address: frank\_hawthorne@umanitoba.ca

Minerals, Nomenclature and Classification, International Mineralogical Association (IMA 2011–56). The holotype specimen of aspedamite has been deposited in the mineral collection of the Department of Natural History, Royal Ontario Museum, catalogue number M56117.

#### GEOLOGY AND OCCURRENCE

The quarry at Herrebøkasa is situated approximately 2 km north–northeast of the village of Aspedammen, lat.  $59^{\circ} 04' 31''$  N, long.  $11^{\circ} 28' 35''$  E, at an altitude of approximately 175 m a.s.l., in the county of Østfold. Geologically, the area belongs to the south Norwegian Precambrian shield, and occurs in the border zone between the Iddefjord granite (~900 Ma) and a gneiss complex (~1800 Ma). Mining of feldspar and quartz in the region dates back to the 1870s, and preliminary lists of minerals and descriptions were published by Brøgger (1881, 1883, 1906) and Blomstrand (1884, 1887), and later documented by Hestmark (1999).

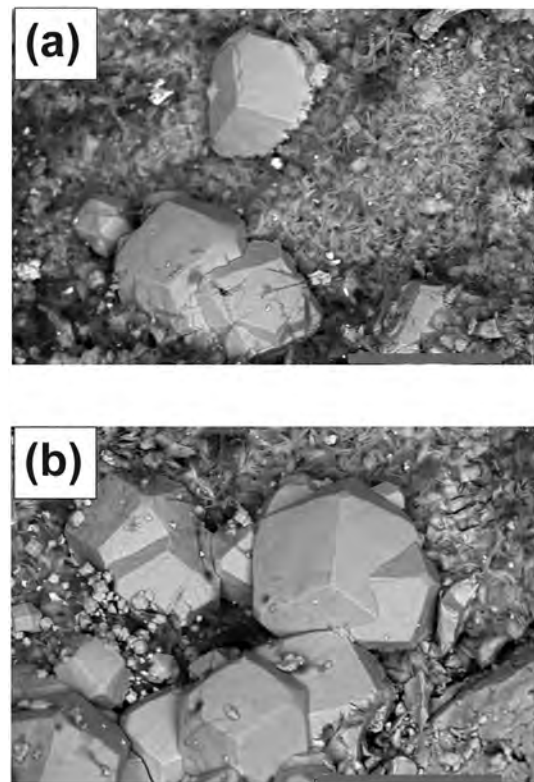


FIG. 1. SEM images of aspedamite: (a) dodecahedra and cube-modified dodecahedron of aspedamite; (b) crystals of aspedamite on a mat of fibrous Al–Nb–Fe–Ti–Ca–K–bearing silicate. The scale bar is 50 micrometers long.

The quarry at Herrebøkasa was opened in 1932, and produced approximately 400 tonnes of feldspar before World War II. After the war, quarrying was sporadic and ceased in 1962.

The exposed part of the pegmatite is 15 m wide and about 100 m long, extending west–southwest and dipping south. The host rocks are granite to the north and gneiss or migmatite to the south. The main minerals are microcline, muscovite and (partly smoky) quartz; plagioclase is fairly scarce. Other minerals include dark green, violet and colorless fluorite, monazite-(Ce), xenotime-(Y), rutile, columbite-(Fe), rynersonite, samarskite, beryl, spessartine, topaz, triplite, bertrandite, fluorapatite, uraninite, thorite and secondary uranium-minerals such as uranophane, kasolite and liandratite (Kristiansen 2006, 2007, 2008, Nilssen 1970), altogether some 40 other species. This is an NYF-family pegmatite, close to the allanite–monazite type of the REL–REE subclass (Černý & Ercit 2005).

#### PHYSICAL PROPERTIES

Aspedamite was found on only one specimen, an altered pyramid-like crystal of monazite,  $12 \times 12 \times 6$  mm, penetrated by broken plates of columbite-(Fe) and muscovite, and labeled H02/99. The top of the crystal, approximately  $2 \text{ mm}^2$ , is covered by a white mat of fibrous Al–Nb–Fe–Ti–Ca–K–bearing silicate upon which are perched small euhedral crystals of aspedamite (Fig. 1a). The dominant form is the dodecahedron {110}; it may be modified by the cube {100} (Fig. 1b). Crystals are up to a maximum of 50  $\mu\text{m}$  across, generally isolated, but in some cases aggregated, where the crystals tend to be intergrown on their edges or cluster together. Aspedamite is brownish orange to deep red with a very pale orange streak and an adamantine luster; it does not fluoresce under ultraviolet light. No cleavage, parting or twinning was observed; the Mohs hardness is 3–4, and the mineral is brittle. The calculated density is  $4.070 \text{ g/cm}^3$ , and the calculated index of refraction is 2.084.

#### RAMAN SPECTROSCOPY

The Raman spectrum is shown in Figure 2. The weak peaks at  $\sim 3460 \text{ cm}^{-1}$  ( $\text{H}_2\text{O}$  and OH stretches) and  $\sim 1610 \text{ cm}^{-1}$  (H–O–H bend) are in accord with the presence of  $\text{H}_2\text{O}$  and OH in the structure of aspedamite. The principal peaks are as follows: 933, w; 865, sh; 812, m; 666, vs; 448, vw; 359, m; 234, s; 169, s; 117, w [vs: very strong; s: strong; m: medium; w: weak; vw: very weak; sh: shoulder]. After Nyman *et al.* (2006), we assign peaks between 700 and  $1000 \text{ cm}^{-1}$  to Nb–O vibrations, and lower-frequency bands to stretching vibrations involving lower-valence cations and to cooperative lattice modes.

## CHEMICAL COMPOSITION

Crystals were analyzed with a Cameca SX-100 electron microprobe operating in the wavelength-dispersion mode with an accelerating voltage of 15 kV, a specimen current of 20 nA, and a beam diameter of 5  $\mu\text{m}$ . The data were reduced with the method of Pouchou & Pichoir (1985) and are given in Table 1. The presence of (OH) and (H<sub>2</sub>O) groups was established by crystal-structure solution and refinement. In addition, the Raman spectra (Fig. 2) indicate a broad band in the region 3450  $\text{cm}^{-1}$  and a relatively sharp band at 1610  $\text{cm}^{-1}$  indicative of H<sub>2</sub>O. Table 1 gives the chemical composition (mean of ten determinations). The calculation of the unit formula will be discussed later.

## X-RAY POWDER DIFFRACTION

X-ray powder-diffraction data were obtained using a Gandolfi attachment mounted on a Bruker D8 rotating-anode Discover SuperSpeed micro-powder diffractometer with a multi-wire 2D detector. X-ray powder-diffraction data (in  $\text{\AA}$  for CuK $\alpha$ ,  $\lambda = 1.54184 \text{\AA}$ ) are given in Table 2. The unit-cell parameter  $a$  was

obtained by least-squares refinement: 12.916(2)  $\text{\AA}$ ,  $V = 2154.7(9) \text{\AA}^3$ .

## CRYSTAL-STRUCTURE SOLUTION AND REFINEMENT

A crystal was attached to a tapered glass fiber and mounted on a Bruker D8 three-circle diffractometer equipped with a rotating-anode generator (MoK $\alpha$ ), multilayer optics and an APEX-II detector. A total of 38,117 intensities (12,584 within the Ewald sphere) was collected to 60° 2 $\theta$  using 20 s per 0.2° frames, with a crystal-to-detector distance of 5 cm. Empirical absorption-corrections (SADABS; Sheldrick 2008) were applied, and equivalent reflections were corrected for Lorentz, polarization and background effects, averaged and reduced to structure factors. The unit-cell dimension was obtained by least-squares refinement of the positions of 9876 reflections with  $I > 10\sigma I$  and is given in Table 3, together with other information pertaining to data collection and structure refinement.

All calculations were done with the SHELXTL PC (Plus) system of programs;  $R$  indices are of the form given in Table 3 and are expressed as percentages. The structure was solved by direct methods and refined to convergence by full-matrix least-squares in the space group  $Im\bar{3}$ . The assignment of scattering species and chemical species to specific sites will be discussed below. Refined coordinates and anisotropic-displacement parameters of all atoms are listed in Table 4, selected interatomic distances are given in Table 5, refined site-scattering values (Hawthorne *et al.* 1995) in Table 6, and bond valences, calculated with the parameters of Brown & Altermatt (1985), are given in Table 7. A table of structure factors and a cif file are available from the Depository of Unpublished Data on

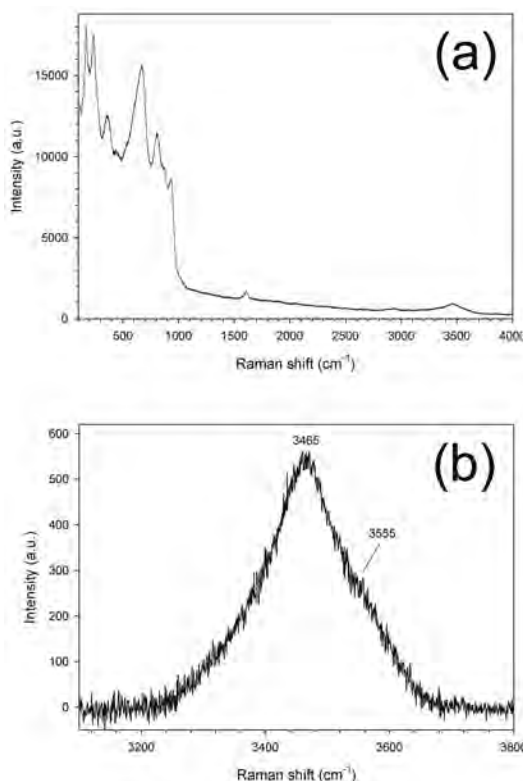


FIG. 2. The Raman spectrum of aspedamite.

TABLE 1. CHEMICAL COMPOSITION OF ASPEDAMITE

Constituent	wt.%	Range	Stand. dev.	Probe standard
Nb <sub>2</sub> O <sub>5</sub>	65.64	64.38 - 66.72	0.60	Ba <sub>2</sub> Nb <sub>2</sub> O <sub>15</sub>
Ta <sub>2</sub> O <sub>5</sub>	1.78	1.41 - 2.31	0.33	MnNb <sub>2</sub> Ta <sub>2</sub> O <sub>9</sub>
SiO <sub>2</sub>	0.78	0.66 - 1.06	0.11	Diopside
ThO <sub>2</sub>	5.64	5.05 - 6.30	0.39	ThO <sub>2</sub>
TiO <sub>2</sub>	2.15	1.95 - 2.31	0.13	Titanite
Fe <sub>2</sub> O <sub>3</sub>	10.56	12.05 - 14.02	0.59	Fayalite
FeO*	2.73	---	---	
MnO	0.82	0.38 - 1.51	0.42	Spessartine
CaO	0.28	0.19 - 0.43	0.06	Diopside
K <sub>2</sub> O	0.16	0.05 - 0.46	0.11	Orthoclase
La <sub>2</sub> O <sub>3</sub>	0.52	0.37 - 0.73	0.11	LaPO <sub>4</sub>
Ce <sub>2</sub> O <sub>3</sub>	1.62	1.41 - 1.85	0.14	CePO <sub>4</sub>
Nd <sub>2</sub> O <sub>3</sub>	0.44	0.31 - 0.62	0.10	NdPO <sub>4</sub>
H <sub>2</sub> O**	7.20			
Total	100.32			

\* calculated from the refined structure;

\*\* calculated from (H<sub>2</sub>O)<sub>6</sub>(OH)<sub>3</sub> derived from the refined structure.

Not detected: F, Na, Mg, Al, P, Sc, V, Cr, Cu, Zn, As, Sr, Y, Zr, Mo, Sb, Te, Ba, Pr, Sm, Eu, Gd, Tb, Dy, Ho, Er, Tm, Yb, Lu, Hf, W, Ti, U.

the Mineralogical Association of Canada website [document Aspedamite CM50\_793].

### CRYSTAL STRUCTURE

Aspedamite is a heteropolyniobate (Nyman 2011) isostructural with menezesite (Atencio *et al.* 2008) and the synthetic compound  $Mg_7(MgW_{12}O_{42})(OH)_4(H_2O)_8$  (Günter *et al.* 1990). Here, we have adopted the site nomenclature for menezesite to facilitate comparison, although we point out that aspedamite has additional sites.

TABLE 2. X-RAY POWDER-DIFFRACTION DATA FOR ASPEDAMITE

$l_{\text{obs}}$	$d_{\text{obs}}$	$d_{\text{calc}}$	$h$	$k$	$l$	$l_{\text{obs}}$	$d_{\text{obs}}$	$d_{\text{calc}}$	$h$	$k$	$l$
100	9.107	9.133	0	1	1	13	2.096	2.095	2	3	5
10	5.279	5.273	1	1	2			2.095	3	2	5
15	4.567	4.567	0	2	2	5	2.042	2.042	2	0	6
15	4.083	4.084	0	1	3			2.042	0	2	6
		4.084	1	0	3	5	1.902	1.904	1	3	6
4	3.726	3.729	2	2	2	5	1.824	1.827	4	3	5
18	3.454	3.452	1	2	3	10	1.790	1.791	4	0	6
		3.452	2	1	3			1.791	0	4	6
28	3.233	3.229	0	0	4	8	1.757	1.758	3	3	6
14	3.046	3.044	1	1	4			1.758	2	5	5
33	2.889	2.888	0	2	4	29	1.726	1.726	2	4	6
		2.888	2	0	4			1.726	4	2	6
9	2.754	2.754	2	3	3	6	1.641	1.640	3	2	7
36	2.635	2.636	2	2	4			1.640	1	5	6
6	2.532	2.533	1	0	5	11	1.615	1.615	0	0	8
		2.533	1	3	4	6	1.591	1.590	1	1	8
		2.533	3	1	4			1.590	1	4	7
3	2.361	2.358	2	1	5			1.590	4	5	5
5	2.211	2.215	3	0	5	2	1.545	1.544	5	3	6
		2.215	3	3	4	3	1.502	1.501	0	5	7
							1.501	4	3	7	

Values of  $d$  are quoted in Å.

### Coordination of cations

**The A site:** The A site is coordinated by six O atoms in a distorted octahedral arrangement with a  $\langle A-O \rangle$  distance of 2.016 Å and a refined site-scattering value of 446(2)  $epfu$  (electrons per formula unit), consistent with occupancy of this site predominantly by Nb.

**The B site:** The B site is coordinated by six O atoms in a regular octahedral configuration with a  $\langle B-O \rangle$  distance of 1.994 Å and a refined site-scattering of 154(1)  $epfu$ . These values are also consistent with occupancy of this site predominantly by Nb.

**The A and B sites:** Together, the A and B sites contain the more highly charged cations of smaller radius [*i.e.*, Nb (0.64 Å), Ta (0.64 Å),  $Ti^{4+}$  (0.605 Å), Si (0.40 Å),  $Fe^{3+}$  (0.645 Å); radii from Shannon 1976]. The occurrence of Si in octahedral coordination in aspedamite is unusual. However, the electron-microprobe results are definitive, and there are no visible inclusions in the grain analyzed. It should be noted that octahedrally coordinated Si does occur in low-pressure minerals, *e.g.*, thumasite, ideally  $Ca_6^{[6]}Si_2(CO_3)_2(SO_4)_2(OH)_{12}(H_2O)_{24}$  (Edge & Taylor 1969). The sum of these penta- and tetravalent cations (excluding Th) in the empirical formula (see section on Chemical Formula below) is

TABLE 3. MISCELLANEOUS CRYSTALLOGRAPHIC DATA FOR ASPEDAMITE

$a$ (Å)	12.9078(6)	crystal size (μm)	40 × 40 × 20
$V$ (Å <sup>3</sup> )	2150.6(3)	radiation	MoKα
Space group	$Im\bar{3}$	total no. of reflections	38117
$Z$	2	no. in Ewald sphere	12584
$D_{\text{calc}}$ (g/cm <sup>3</sup> )	4.070	no. unique reflections	596
$R_{\text{e}}$ (%)	1.6	$R$ (merge) (%)	1.7
$wR_2$ (%)	4.2	no. with $( F_o  > 4\sigma)$	593
$R_1 = \sum( F_o  -  F_c ) / \sum F_o $			
$wR_2 = [\sum w(F_o^2 - F_c^2)^2 / \sum w(F_o^2)^2]^{1/2}$			
where $w = 1 / [\sigma^2(F_o^2) + (0.0237^*P)^2 + 8.8017^*P]$			
$P = (\max(F_o^2, O) + 2^*F_c^2) / 3$			

TABLE 4. COORDINATES AND DISPLACEMENT PARAMETERS (Å<sup>2</sup>) OF ATOMS IN ASPEDAMITE

Site	$x$	$y$	$z$	$U_{\text{eq}}$	$U_{11}$	$U_{22}$	$U_{33}$	$U_{23}$	$U_{13}$	$U_{12}$
A	0	0.11863(2)	0.24177(2)	0.01183(10)	0.01225(14)	0.01213(14)	0.01111(14)	0.00027(8)	0	0
A'	0.1104(15)	½	0.2922(15)	0.039(6)						
B	¼	¼	¼		0.02107(19)	0.02107(19)	0.02107(19)	-0.00159(10)	-0.00159(10)	-0.00159(10)
C'	0	½	0.0245(17)	0.019(2)						
C''	-0.0113(3)	½	0	0.0075(15)						
D	0	0	0	0.00906(15)	0.00906(15)	0.00906(15)	0.00906(15)	0	0	0
E	0.368(2)	0.238(2)	0	0.129(16)						
O(1)	0.20860(11)	0.38757(11)	0.30687(11)	0.0152(4)	0.0165(7)	0.0122(6)	0.0170(7)	-0.0039(5)	-0.0010(5)	-0.0008(5)
O(2)	0.3461(2)	0	0	0.0158(6)	0.0156(13)	0.0169(13)	0.0148(13)	0	0	0
O(3)	0.09985(15)	0	0.17206(15)	0.0120(4)	0.0115(8)	0.0109(8)	0.0136(9)	0	0.0013(7)	0
O(41)	0.4050(11)	0.36468(11)	0	0.034(3)						
O(42)	0.3787(10)	0.3923(11)	0	0.016(3)						
O(43)	0.352(2)	0.425(2)	0	0.052(6)						

TABLE 5. SELECTED INTERATOMIC DISTANCES (Å) AND BOND ANGLES (°) IN ASPEDAMITE

A-O(1)	1.8550(14)	x2	C'-O(2)	2.011(5)	x2	C''-O(2)	1.992(3)	x2
A-O(2)	2.039(2)		C'-O(41)	1.968(14)	x2	C''-O(41)	2.015(9)	x2
A-O(3)	1.957(2)		C'-O(41)	2.329(17)	x2	C''-O(41)	2.253(10)	x2
A-O(3)	2.1944(14)	x2	C'-O(42)	1.870(17)	x2	C''-O(42)	2.001(7)	x2
<A-O>	2.016		C'-O(42)	2.341(19)	x2	C''-O(42)	2.194(8)	x2
A'-O(1)	1.937(13)	x2	C'-O(43)	1.87(2)	x2	C''-O(43)	2.084(18)	x2
A'-O(41)	2.10(2)	x2	C'-O(43)	2.43(3)	x2	C''-O(43)	2.215(17)	x2
A'-O(43)	1.91(3)		B-O(1)	1.9944(14)	x6	D-O(3)	2.5678(19)	x12
<A'-O>	1.997							
E-O(1)	2.77(3)	x2	A-A'	2.229(19)		O(2)-A-O(1)	99.27(6)	x2
E-O(1)	2.848(11)	x2	C'-C'	0.63(4)		O(2)-A-O(3)	75.34(7)	x2
E-O(1)	3.13(2)	x2	C'-C''	0.35(2)		O(3)-A-O(1)	98.08(6)	x2
E-O(2)	3.08(3)		C''-C''	0.29(6)		O(3)-A-O(3)	82.07(9)	x2
E-O(3)	3.09(3)		A'-E	2.33(3)		O(1)-A-O(3)	92.51(6)	x2
E-O(41)	1.71(3)					O(3)-A-O(3)	71.93(9)	
E-O(41)	3.06(3)	x2	O(41)-O(42)	0.49(4)		O(1)-A-O(1)	102.95(9)	
E-O(42)	2.00(3)		O(42)-O(43)	0.55(3)		<O-A-O>	89.12	
E-O(42)	2.66(3)	x2	O(41)-O(43)	1.04(4)				
E-O(43)	2.43(4)							
E-O(43)	2.28(4)	x2	O(1)-B-O(1)	89.46(6)	x6			
			O(1)-B-O(1)	90.54(6)	x6			
			<O-B-O>	90.00				

TABLE 6. REFINED SITE-SCATTERING AND ASSIGNED SITE-POPULATIONS IN ASPEDAMITE

Site	Refined site-scattering (epfu)	Assigned site-population (apfu)	Assigned site-scattering (epfu)	Sum of cations
A	446(2)	Nb <sub>0.643</sub> Ta <sub>0.158</sub> Ti <sub>0.525</sub> Si <sub>0.253</sub> Fe <sup>3+</sup> <sub>0.991</sub>	447.8	11.57
A'	11(2)	□ <sub>11.570</sub> Fe <sup>3+</sup> <sub>0.430</sub>	11.2	0.43
B	154(1)	Nb <sub>3.334</sub> Ta <sub>0.054</sub> Ti <sub>0.182</sub> Si <sub>0.088</sub> Fe <sup>3+</sup> <sub>0.342</sub>	154.8	4
C'	26(4)	Fe <sup>3+</sup> <sub>1.712</sub> Fe <sup>2+</sup> <sub>1.00</sub> □ <sub>0.288</sub>	70.5	3
C''	47(3)			
D	64.3(4)	Th <sub>0.56</sub> Ce <sub>0.146</sub> La <sub>0.047</sub> Nd <sub>0.039</sub> □ <sub>0.207</sub>	64.0	1
E	22(2)	□ <sub>11.295</sub> Mn <sup>2+</sup> <sub>0.304</sub> Ce <sub>0.131</sub> K <sub>0.089</sub> Ce <sub>0.113</sub> La <sub>0.037</sub> Nd <sub>0.030</sub>	22.4	12
Σ	770.3		770.7	

TABLE 7. BOND LENGTHS (Å) AND BOND VALENCES (vu) AROUND THE DISORDERED O(4) ANION IN ASPEDAMITE

	O(41)		O(42)		O(43)				
	Fe <sup>3+</sup>	Fe <sup>2+</sup>	Fe <sup>3+</sup>	Fe <sup>2+</sup>	Fe <sup>3+</sup>	Fe <sup>2+</sup>			
O-C'	1.968	0.57	0.53	1.870	0.74	0.69	1.87	0.74	0.69
O-C'	2.329	0.21	0.20	2.341	0.21	0.19	2.43	0.16	0.15
O-C''	2.015	0.50	0.41	2.001	0.52	0.49	2.084	0.42	0.39
O-C''	2.253	0.26	0.25	2.194	0.31	0.29	2.215	0.29	0.27
	Fe <sup>3+</sup>	Mn <sup>2+</sup>	Fe <sup>3+</sup>	Mn <sup>2+</sup>	Fe <sup>3+</sup>	Mn <sup>2+</sup>			
O-A' × 2	2.10	0.40	--	2.20	0.30	--	1.91	0.66	--
O-E	1.71	--	--	2.00	--	0.57	2.43	--	0.18
O-E × 2	3.06	--	0.03	2.66	--	0.10	2.28	--	0.27

14.24 *apfu* (atoms per formula unit), and full occupancy of the *A* and *B* sites requires 16 *apfu*. We have filled the *A* and *B* sites by assigning 1.76 *apfu*  $\text{Fe}^{3+}$  to these sites. The difference in mean bond-length between the two octahedra is 0.022 Å, and the scattering difference is less than 4%. With the large number of constituents, it is not possible to convincingly assign distinct site-populations to *A* and *B*, and we have assigned Nb, Ta,  $\text{Ti}^{4+}$ , Si and  $\text{Fe}^{3+}$  equally to each site. We recognize that this distribution of cations is only an approximation; however, it results in both the *A* and *B* sites containing more than 80% Nb, and any adjustment of the occupancies of the minor cations cannot produce anything other than dominance by Nb at both sites. The site scattering at each of the *A* and *B* sites was modeled by a variable occupancy-factor for Nb, and the results are in accord with the proposed disorder among cations.

*The A'* site: At the latter stages of refinement, there was a small residual peak in the difference-Fourier map. This was inserted into the refinement as a possible new cation-site [*i.e.*, not reported previously for either menezesite or  $\text{Mg}_7(\text{MgW}_{12}\text{O}_{42})(\text{OH})_4(\text{H}_2\text{O})_8$ ]. The refined site-scattering value is 11(2) *epfu*. The site is surrounded by five O atoms arranged in a square pyramid with a  $\langle A'-\text{O} \rangle$  distance of 1.997 Å. The identity of this cation is not known; however, the  $\langle A'-\text{O} \rangle$  distance of 1.997 Å is compatible with occupancy by  $\text{Fe}^{3+}$ , and this cation is available in the formula for such an assignment. Thus we refined the occupancy of this site in terms of Fe, obtaining a site population of 0.43  $\text{Fe}^{3+}$  *apfu*. The  $A'-A$  separation is 2.229(19) Å and hence mutual local occupancy of the *A* and *A'* sites is not expected; thus the sum of the cations at the *A* + *A'* sites cannot exceed 12 *apfu*.

*The C* site: The *C* site in both menezesite and  $\text{Mg}_7(\text{MgW}_{12}\text{O}_{42})(\text{OH})_4(\text{H}_2\text{O})_8$  occurs at (0,½,0), and the constituent atoms show large anisotropic displacements, with  $U_{11}$  and  $U_{33}$  2.6–3.3 times greater than  $U_{22}$ . In aspedamite, the  $U_{11}/U_{22}$  and  $U_{33}/U_{22}$  values are 3.1 and 4.0, respectively, and we refined two “split” positions, *C* and *C'*, both disordered off the special position (0,½,0) and lying on the (010) mirror plane. Locally, only one of the four possible (*i.e.*, two *C* and two *C'*) positions can be occupied because of the short separations of the sites (Table 5). There are two adjacent O(2) anions, one above and the other below the (010) mirror plane, and within the mirror are four equatorial anions that complete the octahedral coordination. In both menezesite and  $\text{Mg}_7(\text{MgW}_{12}\text{O}_{42})(\text{OH})_4(\text{H}_2\text{O})_8$ , the large anisotropy observed for the equatorial anion was modeled as a split site, with the occupancy factors for each set at 0.5. We also observed similar large displacements for this anion, and modeled it as three distinct sites with freely refining positional, isotropic-displacement and occupancy parameters. An electron-density map within the (010) mirror plane shows continuous elliptical electron-density for both the (0,½,0) position

and the equatorial anion, and we modeled both sites as “split” sites in order to extract more detailed information on short-range order and local bond-lengths. The split-site model and the simple anisotropic model result in the same *R* indices, and the anisotropic model gave a  $\langle C-\text{O} \rangle$  distance of 2.06 Å and a refined site-scattering of 24.0(2) *epfu*, consistent with a site dominated by Fe, with  $\text{Fe}^{3+}/(\text{Fe}^{3+} + \text{Fe}^{2+}) \approx 0.67$  (see section on Chemical Formula below).

*The D* site: The *D* site occurs at the center of a large cage formed by twelve face- and corner-sharing *A* octahedra. The observed site-scattering of 64.3(4) *epfu* is consistent with occupancy primarily by Th (as indicated by the chemical formula), and this scattering factor was used in the refinement. The [12]-coordination and  $\langle D-\text{O} \rangle$  distance of 2.568 Å are consistent with this assignment.

*The E* site: The *E* site is [11]-coordinated, is dominated by vacancy (~11.3  $\square$  out of a total of 12 constituents *pfu*), and contains a large variety of minor accessory cations. The refined site-scattering is only 22(2) *epfu*, and the isotropic-displacement parameter is very large. It is surrounded by 17 anions at distances from 1.71 to 3.13 Å (Table 5). However, the O(41), O(42) and O(43) anions are separated by ~0.5 and ~1 Å, and only one of these three sites can be locally occupied, reducing the true coordination number of the *E* site to [11]. It is probable that the *E* cations show significant positional disorder as a function of the short-range occupancy of the O(41), O(42) and O(43) sites and the identity of the specific *E* cation, but this cannot be derived from the refinement because of the low occupancy of the *E* site.

#### Bond topology

The key building block of the aspedamite structure is the heteropolyanion  $[\text{DA}_{12}\text{O}_{42}]$ ; it consists of twelve face- and corner-sharing  $\text{AO}_6$  octahedra that surround the [12]-coordinated *D* cation. Two  $\text{AO}_6$  octahedra share a face through their O(2)–O(3)–O(3) vertices to form an  $[\text{A}_2\text{O}_9]$  dimer. Six of these dimers link by sharing O(3) vertices (four per dimer) (Fig. 3) to form a compact cluster. The twelve O(3) anions that form the innermost anion shell of the polyanion are coordinated to the central *D* cation to form the  $[\text{DA}_{12}\text{O}_{42}]$  heteropolyanion. This type of heteropolyanion was originally described by Dexter & Silverton (1968).

There are eight heteropolyanions at the corners of the unit cell, with an additional heteropolyanion at the center, forming an *I*-centered arrangement. Each heteropolyhedral cluster is decorated by eight *B* octahedra, each of which bridges two adjacent clusters along the body diagonals of the cell by sharing three O(1) anions with each cluster (Fig. 4). Further intercluster linkage is provided by the *C* octahedra that link pairs of adjacent clusters in the *a* direction by sharing an O(2)

anion with each cluster (Fig. 4). The *A'* and *E* cations occur around the *C* octahedron (Fig. 4). The *A'* cation is coordinated by five O atoms in a square-pyramidal arrangement, and shares an O(1)–O(1) edge with the *A* octahedron (Fig. 5).

#### Short-range order involving the O(4) and *C* sites

As mentioned above, we modeled the electron density in the vicinity of the *C* site (0, 1/2, 0) as two distinct sites, *C'* and *C''*, and the electron density associated with the O(4) anion as three distinct sites, O(41), O(42) and O(43). Such “split-site” models give more quantitative information on short-range effects in the structure than does modeling of the scattering using anisotropic-displacement parameters. This issue is of particular interest in aspedamite as the details regarding the local arrangements of O(4) and *C* are related to the content of  $[\text{H}_2\text{O}, (\text{OH})]_{12}$  in the formula unit. The positional disorder is contained within the mirror plane that bisects the *C* octahedron midway between the two O(2) vertices (Fig. 6). The O(4) site is split largely tangentially to the equatorial plane of the *C* octahedron. The *C'* site is displaced further from (0 1/2 0) than the *C''* site, resulting in *C'*–O(4)\* distances that show more dispersion (1.87–2.43 Å) than the *C''*–O(4)\* distances (1.99–2.25 Å) (Table 5).

The O(4) anion contributes twelve  $[\text{H}_2\text{O} + (\text{OH})]$  *apfu*; the details of the local order that indicate the relative  $\text{H}_2\text{O}$  and (OH) contents are of interest in this structure type. The coordination of the O(41) site is shown in Figure 7; the coordinations of O(42) and O(43) are qualitatively similar and are not shown. What is immediately apparent in Figure 7 is the fact that the two *C'* and two *C''* sites are all very close together (0.29–0.63 Å separations, Table 5) and hence a maximum of one of these four sites can locally be occupied. The bond lengths and corresponding bond-valences around the O(41), O(42) and O(43) sites are listed in Table 7. The central O(41,42,43) anions receive one bond-valence contribution from the *C'* or *C''* sites, and this varies from 0.00 (for a vacancy) to 0.74 *vu* [from  $\text{Fe}^{3+}$  at *C'* bonded to O(43), Table 7]. The *A'* and *E* sites are dominated by vacancies (Table 6), but have low occupancies of cations that we approximate by  $\text{Fe}^{3+}$  at *A'* and  $\text{Mn}^{2+}$  at *E*. Obviously, there are large numbers of possible local arrangements of bond valences. Some of these are compatible with occupancy of O(4) by (OH): *e.g.*, O(41)–*C'* $\text{Fe}^{3+}$  = 0.57, O(41)–*A'* $\text{Fe}^{3+}$  = 0.40, O(41)–*E* $\text{Mn}^{2+}$  = 0.03,  $\Sigma$  = 1.00 *vu*; O(41)–*C''* $\text{Fe}^{2+}$  = 0.25, O(41)–*A'* $\text{Fe}^{3+}$  = 0.40  $\times$  2,  $\Sigma$  = 1.05 *vu*; O(42)–*C'* $\text{Fe}^{3+}$  = 0.74, O(42)–*A'* $\text{Fe}^{3+}$  = 0.30,  $\Sigma$  = 1.04 *vu*; O(42)–*C''* $\text{Fe}^{2+}$  = 0.49, O(42)–*E* $\text{Mn}^{2+}$  = 0.57,  $\Sigma$  = 1.06 *vu*; O(43)–*C''* $\text{Fe}^{3+}$  = 0.74, O(43)–*E* $\text{Mn}^{2+}$  = 0.27,  $\Sigma$  = 1.01 *vu*; O(43)–*C''* $\text{Fe}^{2+}$  = 0.39, O(43)–*A'* $\text{Fe}^{3+}$  = 0.66,  $\Sigma$  = 1.01 *vu*. It is apparent that the anion at O(41,42,43) must receive bond valence from *C'* or *C''* and either *A'* or *E* (or both), in order for

O(41,42,43) to be occupied by an (OH) group. Where a particular *A'* site is occupied, three adjacent O(4) sites receive a bond-valence contribution, and where a particular *E* site is occupied, up to three adjacent O(4) sites may receive a significant bond-valence contribution. The total *A'* + *E* cation content is  $0.43 + 0.70 = 1.13$  *apfu*, and this constrains an upper limit of 3.39 (1.13  $\times$  3) *apfu* (OH) at the O(4) site. The error associated with the cation content at the *A'* + *E* sites is significant, and we regard this value of 3.39 (OH) *apfu* as an upper limit that should be used as a guideline. In summary, the anion chemistry  $[(\text{OH}), \text{H}_2\text{O}]$  at the O(4) site varies as a function of the cooperative *C'*, *C''*, O(41,42,43), *A'* and *E* site-occupancies and local positional order, and the limiting criteria for (OH) in aspedamite are linked to the minor cation content at the *A'* and *E* sites.

#### THE CHEMICAL FORMULA OF ASPEDAMITE

Aspedamite occurs as minute crystals (a few tens of micrometers in size) in extremely low overall abundance, and direct determination of  $\text{H}_2\text{O}$  content and Fe valence is not possible. Approaching the chemical composition from a crystal-chemical viewpoint, there are the following issues: (1) a variable anion composition that falls somewhere between  $\text{O}_{42}(\text{H}_2\text{O})_{12}$  and  $\text{O}_{42}(\text{OH})_{12}$ ; (2) the presence of significant Fe of unknown valence state(s); (3) the presence of a large variety of cations with extensive solid-solution; (4) significant positional disorder of both cations and anions; (5) an uncertain total number of cations in the chemical formula. Because of the complexities involved in ascertaining the correct formula for aspedamite, we used the same single crystal for structure refinement, electron-microprobe analysis and Raman spectroscopy in order to remove any possible errors resulting from compositional heterogeneity in the sample.

First, some qualitative considerations. Aspedamite is brownish orange to red, and we can infer the presence of  $\text{Fe}^{3+}$  as a necessary chromophore. Moreover, the occurrence of aspedamite in an alteration assemblage suggests an oxidizing environment. Thus it seems reasonable to infer that significant  $\text{Fe}^{3+}$  is present in aspedamite. It has been proposed that heteropolyniobates form under relatively alkaline conditions (Nyman *et al.* 2002), and  $\text{H}_2\text{O}$  is likely to dominate over (OH) at the complex-anion site. The inferred dominance of  $\text{H}_2\text{O}$  over OH in aspedamite is in accord with the Raman spectra acquired on the X-ray single crystal (Fig. 2).

Next, let us consider the high-charge cations in aspedamite:  $\text{Nb}^{5+} + \text{Ta}^{5+} + \text{Ti}^{4+} + \text{Si}^{4+}$  together with  $\text{Fe}^{3+}$  and  $\text{Fe}^{2+}$ . There are three octahedrally coordinated sites, *A*, *B* and *C*, and one [5]-coordinated site, *A'*, that may be occupied by Fe. We assigned  $(\text{Nb}^{5+} + \text{Ta}^{5+} + \text{Ti}^{4+} + \text{Si}^{4+})$  to the *A*, *A'* and *B* sites on the basis of their refined site-scattering values, mean bond-lengths and the availability of these cations in the empirical

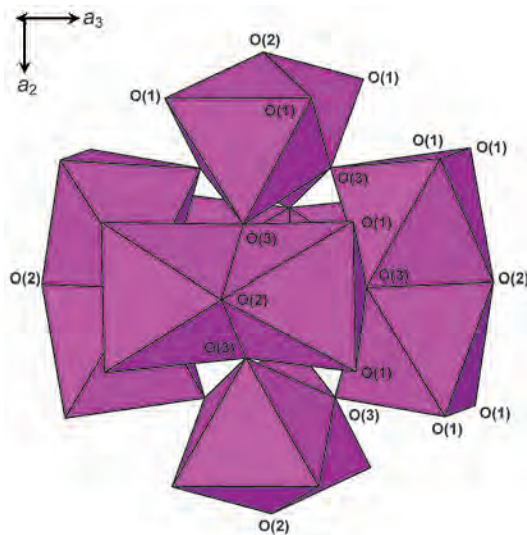


FIG. 3. The  $[DA_{12}O_{42}]$  heteropolyanion in aspedamite;  $AO_6$  octahedra are pink, the central  $D$  cation is hidden. Projected down an axis rotated slightly from [100].

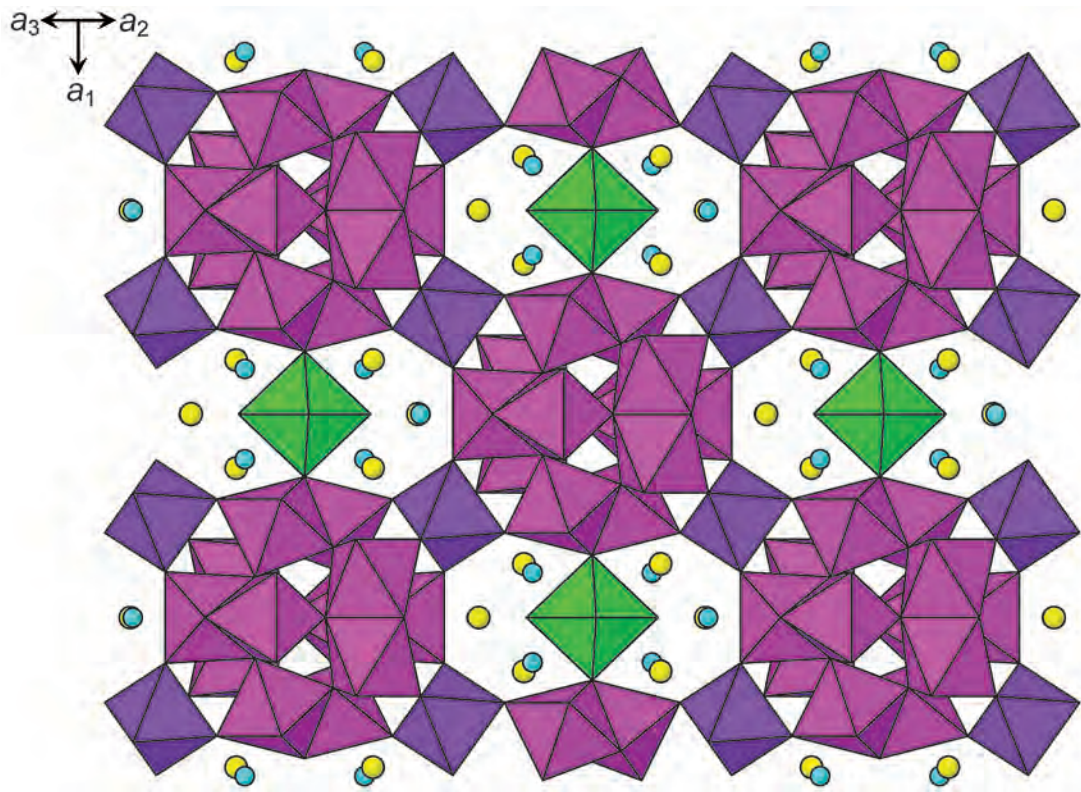


FIG. 4. Connectivity of the  $[DA_{12}O_{42}]$  heteropolyanions (pink) along [100] via  $C$  octahedra (green) at the  $O(2)$  anions and along [111] via  $B$  octahedra (purple) at the  $O(1)$  anions in aspedamite.  $A'$  cations: blue circles,  $E$  cations: yellow circles. Projected onto (011).

FIG. 5. The  $A'$  square pyramid (blue) flanking the  $A$  octahedra (pink) in aspedamite. Projected down an axis rotated slightly from [010].

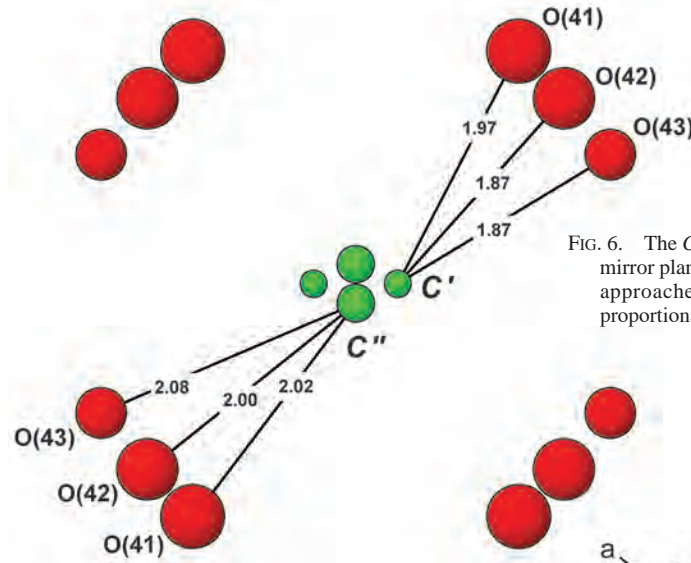
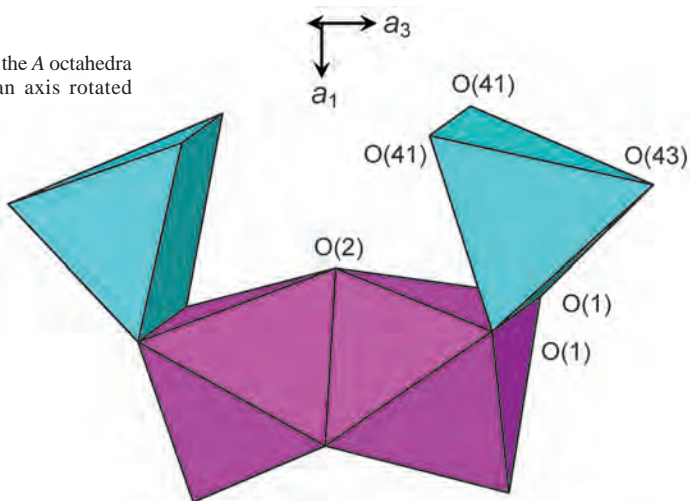


FIG. 6. The  $C$  and  $O(4)$  sites disordered within the equatorial mirror plane of the  $C\phi_6$  octahedron in aspedamite. Shorter approaches ( $\text{\AA}$ ) are labeled. Shaded circle areas are proportional to the refined occupancies.

FIG. 7. The coordination of the  $O(41)$  anion (yellow circle). There are two  $C'$  and two  $C''$  sites coordinating this anion; however, only one of these sites may be occupied by a cation, as their separations are in the range 0.29–0.63  $\text{\AA}$ . The coordinations of the  $O(42)$  and  $O(43)$  sites are similar.

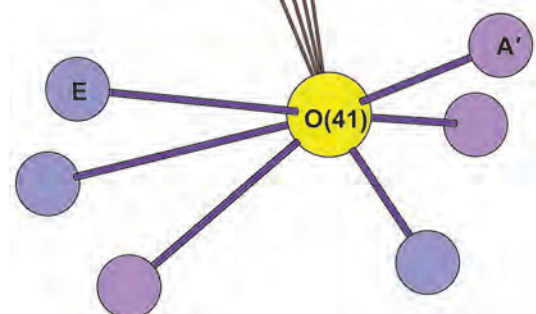


TABLE 8. COMPARISON OF SIMPLIFIED CHEMICAL FORMULAE (apfu) OF ASPEDAMITE AND MENEZESITE

$(A + B)_{16}$	Nb	Ti	Zr	$Fe^{3+}$	Ta	Si	Th	$\langle Z^+ \rangle$	Approx. content			
Aspedamite	13.0	0.7	—	1.8	0.2	0.3	—	75.4	$[Nb_{13}TiFe^{3+}]^{75+}$			
Menezesite	9.2	3.3	2.7	—	0.4	0.1	0.3	73.6	$[Nb_{10}Ti_3Zr_3]^{74+}$			
Simplified formulae												
Sites	$E_{12}$	$D$	$C_3$	$B_4$	$A_{12}$	O(4)						
Aspedamite	$\square_{12}$	Th	$Fe^{3+}_2Fe^{2+}$	$Nb_4$	$Nb_2Fe^{3+}_2Ti$	$O_{42}$	$(H_2O)_8(OH)_3$					
Menezesite	$\square_{9.5}Ba_{2.5}$	Ba	$\square_{1.5}Mg_{1.5}$	$Zr_3Ti$	$Nb_{10}Ti_2$	$O_{42}$	$(H_2O)_{12}$					
End-member compositions relevant to aspedamite												
Aspedamite [1]	$\square_{12}$	Th	$Fe^{3+}_3$	$Nb_4$	$Nb_{12}$	$O_{42}$	$(OH)_9(H_2O)_3$					
Aspedamite [2]	$\square_{12}$	Th	$Fe^{2+}_3$	$Nb_4$	$Nb_{12}$	$O_{42}$	$(OH)_8(H_2O)_6$					
Aspedamite [3]	$\square_{12}$	Th	$Fe^{3+}_3$	$Nb_4$	$Nb_{7.5}Fe^{3+}_{4.5}$	$O_{42}$	$(H_2O)_{12}$					
Aspedamite [4]	$\square_{12}$	Th	$Fe^{2+}_3$	$Nb_4$	$Nb_2Fe^{3+}_3$	$O_{42}$	$(H_2O)_{12}$					
Aspedamite [5]	$\square_{12}$	Th	$Fe^{3+}_3$	$Nb_4$	$Nb_3Ti_9$	$O_{42}$	$(H_2O)_{12}$					
Aspedamite	$= [1] \times 1/3 + [3] \times 2/9 + [4] \times 1/3 + [5] \times 1/9$											
Menezesite end-member compositions												
Menezesite [1]	$\square_6Ba_3$	Ba	$\square_3$	$Zr_4$	$Nb_{12}$	$O_{42}$	$(H_2O)_{12}$					
Menezesite [2]	$\square_6Ba_3$	Ba	$\square_3$	$Ti_4$	$Nb_{12}$	$O_{42}$	$(H_2O)_{12}$					
Menezesite [3]	$\square_{12}$	Ba	$Mg_3$	$Zr_4$	$Nb_{12}$	$O_{42}$	$(H_2O)_{12}$					
Menezesite [4]	$\square_6Ba_6$	Ba	$Mg_3$	$Zr_4$	$Ti_{12}$	$O_{42}$	$(H_2O)_{12}$					
Menezesite	$= [1] \times 1/4 + [2] \times 1/4 + [3] \times 1/3 + [4] \times 1/6$											

TABLE 9. COMPARISON OF SELECTED PROPERTIES OF ASPEDAMITE AND MENEZESITE

	Aspedamite	Menezesite
Formula	$\square_{12}(Fe^{3+},Fe^{2+})_8Nb_4$ [Th(Nb,Fe <sup>3+</sup> ) <sub>12</sub> O <sub>42</sub> ] (H <sub>2</sub> O) <sub>8</sub> (OH) <sub>3</sub>	$Ba_2MgZr_4$ [BaNb <sub>12</sub> O <sub>42</sub> ] (H <sub>2</sub> O) <sub>12</sub>
Symmetry	Cubic	Cubic
Space group	$Im\bar{3}$	$Im\bar{3}$
$a$ (Å)	12.908	13.017
$Z$	2	2
D (g cm <sup>-3</sup> )	4.070	4.181
Color	Brownish orange	Reddish brown
Cleavage	None	None
Hardness	3–4	4
Index of refraction (calc.)	2.084	2.034
Occurrence	Granitic pegmatite	Carbonatite–pyroxenite contact zone

formula of aspedamite. The difference between the sum of the sites and the sum of these cations, *i.e.*,  $16 - (Nb^{5+} + Ta^{5+} + Ti^{4+} + Si^{4+})$ , was assigned as  $Fe^{3+}$  occupying these sites. In  $Mg_7(MgW_{12}O_{42})(OH)_4(H_2O)_8$ , the  $C$  site is occupied by  $Mg$ , and  $\langle C-O \rangle$  is 2.097 Å; if we subtract the  $[^{16}Mg]$  radius value of 0.72 Å from the mean bond-length, we obtain a radius for oxygen of 1.38 Å. When we subtract 1.38 Å from the  $\langle C-O \rangle$  distance, 2.06 Å in aspedamite [single-site  $C$  and  $O(4)$

model], we obtain an aggregate-cation radius of 0.68 Å. In aspedamite, there is no  $Mg$ ,  $\sim 0.30 Mn^{2+}$  apfu and significant  $Fe$  to consider assigning to the  $C$  site. If the  $C$  site in aspedamite were fully occupied by  $Fe$  and  $Mn$ , this would result in  $Fe_{2.70}Mn_{0.30}$  with an effective site-scattering value of 77.7  $epfu$ . Site-scattering refinement for aspedamite gave a value of 71.9(6)  $epfu$  for the  $C$  site for the single-site model; the “split-site” model gave statistically the same value with a much lower precision because of high correlations in the refinement. Hence we will use the more accurate value from the single-site refinement. Clearly, the scattering observed at the  $C$  site is less than that required for complete occupancy by  $Fe$  and  $Mn$ ; there must be another constituent at the  $C$  site with a smaller scattering value than that of  $Fe$  and  $Mn$ . In menezesite,  $(\square_{1.6}Mg_{0.93}Fe^{2+}_{0.23}Mn^{2+}_{0.23})$  apfu was assigned to the  $C$  site, which has a  $\langle C-O \rangle$  distance of 2.143 Å. We are not able to assess the relation between assigned aggregate radii and observed  $\langle C-O \rangle$  in menezesite owing to the dominant vacancy. However, the presence of major vacancies at the  $C$  site in menezesite is important, as (1) it suggests that vacancy is a candidate for the other constituent at the  $C$  site mentioned above, and (2) it indicates that it is inappropriate to normalize the chemical data on a fixed sum of octahedrally coordinated cations to produce the chemical formula. Hence we assigned minor vacancy to the  $C$  site. To do this, we adjusted the  $Fe^{3+}/(Fe^{3+} + Fe^{2+})$  ratio

such that (1) the effective scattering from the assigned site-populations is close to the refined value; (2) the aggregate radius of the assigned constituent-cations is close to that calculated from the observed  $\langle C-O \rangle$  distance in aspedamite; (3) the sum of the oxides in the chemical composition is close to 100 wt%; (4) the effective scattering-values for the remaining sites are close to their refined values. The closest fit to these criteria gave an  $Fe^{3+}/(Fe^{3+} + Fe^{2+})$  ratio of  $\sim 2/3$  at the  $C$  site, an anion composition of  $(H_2O)_9(OH)_3$  at the  $O(4)$  site, and a  $C$ -site composition of  $(Fe^{3+})_{1.712}Fe^{2+}_{1.000}\square_{0.288}$  *apfu*, which gives an aggregate cation-radius of 0.69 Å (disregarding the minor vacancy) and an effective site-scattering value of 71 *epfu*. These are in close accord with the calculated radius of 0.68 Å and the observed site-scattering value of 71.9(6) *epfu*.

All Th was assigned to the  $D$  site, together with sufficient rare-earth elements to accord with the refined site-scattering value (Table 6). All Mn was assigned to the  $E$  site, together with the remaining REE, all Ca and K. The empirical formula of aspedamite on the basis of 54 anions with  $Fe^{3+}/(Fe^{3+} + Fe^{2+}) = 0.67$  and  $O(4) = (H_2O)_9 + (OH)_3$  is  $K_{0.09}Ca_{0.13}Ce_{0.26}La_{0.08}Nd_{0.07}Fe^{2+}_{1.00}Mn_{0.30}Fe^{3+}_{3.48}Th_{0.56}Ti^{4+}_{0.71}Si_{0.34}Nb_{12.98}Ta_{0.21}O_{42}(H_2O)_9(OH)_3$ .

#### COMPARISON OF ASPEDAMITE AND MENEZESITE

The chemical compositions of aspedamite and menezesite are compared on a site basis in Table 8. First, the cations occupying the  $(A + B)_{16}$  sites are given to one decimal place, and then approximated in terms of the three dominant cations in each mineral,  $(Nb, Ti, Fe^{3+})$  in aspedamite and  $(Nb, Ti, Zr)$  in menezesite. Note that the aggregate charge at the  $A$  and  $B$  sites is different in the two minerals:  $\sim 75+$  in aspedamite and  $\sim 74+$  in menezesite. Next, we write simplified empirical formulae for aspedamite and menezesite below. In menezesite,  $C$  is approximately equal to  $\square_{1.57}Mg_{0.94}Mn_{0.23}Fe_{0.23}Al_{0.03}$ , and  $E$  is approximately equal to  $\square_{9.34}Ba_{1.47}K_{0.53}Ca_{0.31}Ce_{0.17}Nd_{0.10}Na_{0.06}La_{0.02}$ ; we may approximate the occupancies of these sites in terms of the two dominant cations at each site as follows:  $C \approx \square_{1.5}Mg_{1.5}$  and  $E \approx \square_{9.5}Ba_{2.5}$ . Here, the principal differences between the simplified empirical formulae of the two minerals are apparent: (1) occupancy of the  $D$  site by Th in aspedamite and by Ba in menezesite; (2) occupancy of the  $C$  site by  $Fe^{3+}_2Fe^{2+}$  in aspedamite and by  $\square_{1.5}Mg_{1.5}$  in menezesite; (3) occupancy of the  $B$  site by  $Nb_4$  in aspedamite and by  $Zr_3Ti$  in menezesite.

Let us next consider the most important end-member constituents in aspedamite. Hawthorne (2002) showed that an end-member composition must conform to the following criteria: (1) The composition must be fixed; (2) the composition must be compatible with the associated crystal-structure; (3) an end-member composition may have two types of cation or anion at one site only if required by the constraint of electroneutrality.

Thus we may consider the simplified compositions of aspedamite and menezesite (Table 8) and evaluate site-by-site the end-members required to represent these simplified compositions; these end members are listed in Table 8. First, let us consider aspedamite. There are five end-member compositions that are relevant to the simplified composition, listed as [1] to [5] in Table 8 and all having one site occupied by two species. The simplified composition of aspedamite may be formed by four of these end-members combined in the amounts indicated in Table 8. End-members [1] and [4] are dominant and occur in equal amounts, and we will write the ideal formula as intermediate between end-members [1] and [4]:  $\square_{12}(Fe^{3+}, Fe^{2+})_3Nb_4[Th(Nb, Fe^{3+})_{12}O_{42}](H_2O, OH)_{12}$ .

For menezesite, there are four significant end-members (Table 8), which combine in the proportions indicated to give the simplified formula. The dominant end-member composition of menezesite is thus composition [3]:  $\square_{12}Mg_3Zr_4[BaNb_{12}O_{42}](H_2O)_{12}$ .

Selected properties of these minerals are listed in Table 9. No physical property can easily distinguish between aspedamite and menezesite. Distinguishing between these two minerals requires (at least) chemical analysis, particularly as the discussion of the chemical compositions of aspedamite and menezesite given above suggest that many other compositionally distinct phases with the same structure should exist.

#### ACKNOWLEDGEMENTS

The non-Černý authors dedicate this paper to the Černý author to recognize his major contributions to Pegmatology, and, for FCH, to acknowledge with thanks almost 40 years of collaborative work in Mineralogy. RK is indebted to Franz Bernhard, Technical University of Graz, for the preliminary EDS-SEM analysis. We thank Harald Folvik, Natural History Museum, University of Oslo, for the scanning electron micrograph photos of aspedamite. This work was supported by a Canada Research Chair in Crystallography and Mineralogy and by Natural Sciences and Engineering Research Council of Canada Discovery, Equipment and Major Installation grants of the Natural Sciences and Engineering Research Council of Canada, and by Innovation grants from the Canada Foundation for Innovation to FCH.

#### REFERENCES

ATENCIO, D., COUTINHO, J.M.V., DORIGUETTO, A.C., MASCARENHAS, Y.P., ELLENA, J. & FERRARI, J.C. (2008): Menezesite, the first natural heteropolyoniobate, from Cajati, São Paulo, Brazil: description and crystal structure. *Am. Mineral.* **93**, 81-87.

BLOMSTRAND, C.W. (1884): Om et uranmineral från trakten af Moss samt de nativa uranaterna i almänhet. *Geol. Fören. Stockholm Förh.* **7**, 59-101 (in Swedish).

BLOMSTRAND, C.W. (1887): Analys af cer- och ytter-fosfater från söndra Norge, ett bidrag till frågan om dessa mineralers kemiska byggnad. *Geol. Fören. Stockholm Förh.* **9**, 160-187 (in Swedish).

BROWN, I.D. & ALTERMATT, D. (1985): Bond-valence parameters obtained from a systematic analysis of the inorganic crystal structure database. *Acta Crystallogr.* **B41**, 244-247.

BRØGGER, W.C. (1881): Nogle bemærkninger om pegmatittgangene ved Moss og deres mineraler. *Geol. Fören. Stockholm Förh.* **5**, 326-376 (in Norwegian).

BRØGGER, W.C. (1883): Om uranbegerts og xenotim fra norske forekomster. *Geol. Fören. Stockholm Förh.* **6**, 744-752 (in Norwegian).

BRØGGER, W.C. (1906): Die Mineralien der Südnorwegischen granitpegmatitgänge. I. Niobate, tantalate und titanoniobate. *Ved. Selsk. Skr. Math.-Naturv.* **6**, 1-162.

ČERNÝ, P. & ERCIT, T.S. (2005): The classification of granitic pegmatites revisited. *Can. Mineral.* **43**, 2005-2026.

DEXTER, D.D. & SILVERTON, J.V. (1968): A new structural type for heteropoly anions. The crystal structure of  $(\text{NH}_4)_2\text{H}_6(\text{CeMo}_{12}\text{O}_{42})12\text{H}_2\text{O}$ . *J. Am. Chem. Soc.* **90**, 3589-3590.

EDGE, R.A. & TAYLOR, H.F.W. (1969): Crystal structure of thaumasite, a mineral containing  $[\text{Si}(\text{OH})_6]^{2-}$  groups. *Nature* **224**, 363-364.

GÜNTER, J.R., SCHMALLE, H.W. & DUBLER, E. (1990): Crystal structure and properties of a new magnesium heteropolytungstate,  $\text{Mg}_7(\text{MgW}_{12}\text{O}_{42})(\text{OH})_4(\text{H}_2\text{O})_8$ , and the isostructural compounds of manganese, iron, cobalt and nickel. *Solid State Ionics* **43**, 85-92.

HAWTHORNE, F.C. (2002): The use of end-member charge-arrangements in defining new mineral species and heterovalent substitutions in complex minerals. *Can. Mineral.* **40**, 699-710.

HAWTHORNE, F.C., UNGARETTI, L. & OBERTI, R. (1995): Site populations in minerals: terminology and presentation of results of crystal-structure refinement. *Can. Mineral.* **33**, 907-911.

HESTMARK, G. (1999): Vitenskap og nasjon: Waldemar Christopher Brøgger 1851-1905. Aschehoug, Oslo, Norway (in Norwegian).

KRISTIANSEN, R. (2006): Liandratitt –  $\text{U}^{6+}(\text{Nb},\text{Ta})_2\text{O}_8$  – fra Herrebøkasa, Østfold. *Stein* **33**(2), 28 (in Norwegian).

KRISTIANSEN, R. (2007): Sekundære Uran-mineraler i Norge. *Norsk Bergverksmus., Skrift* **35**, 49-59 (in Norwegian).

KRISTIANSEN, R. (2008): Nye mineralfunn i Norge. *Stein* **35**(1), 17-21 (in Norwegian).

NILSEN, B. (1970): Samarskites. Chemical composition, formula and crystalline phases produced by heating. *Norsk. Geol. Tidsskr.* **59**, 357-373.

NYMAN, M. (2011): Polyoxoniobate chemistry in the 21st century. *Dalton Trans.* **40**, 8049-8058.

NYMAN, M., BONHOMME, F., ALAM, T.M., RODRIGUEZ, M.A., CHERRY, B.R., KRUMHANSL, J.L., NENOFF, T.M. & SATTLER, A.M. (2002): A general synthetic procedure for heteropolyoniobates. *Science* **297**, 996-998.

NYMAN, M., CELESTIAN, A.J., PARISE, J.B., HOLLAND, G.P. & ALAM, T.M. (2006): Solid-state structural characterization of a rigid framework of lacunary heteropolyoniobates. *Inorg. Chem.* **45**, 1043-1052.

POUCHOU, J.L. & PICHOIR, F. (1985): "PAP"  $\phi(\rho Z)$  procedure for improved quantitative microanalysis. In *Microbeam Analysis* (J.T. Armstrong, ed.). San Francisco Press, San Francisco, California (104-106).

SHANNON, R.D. (1976): Revised effective ionic radii and systematic studies of interatomic distances in halides and chalcogenides. *Acta Crystallogr.* **A32**, 751-767.

SHELDICK, G.M. (2008): A short history of *SHELX*. *Acta Crystallogr.* **A64**, 112-122.

Received November 28, 2011, revised manuscript accepted June 12, 2012.